The Disorder of Mitochondrial Dynamics Causes Deafness By Promoting Macrophage-Mediated Hair Cell Death

Yuan Zhang
Southeast University
Xiaolong Fu (fuxiaolongshifan@163.com)
Southeast University https://orcid.org/0000-0002-3884-0916
Yiyuan Li
Southeast University
Guodong Hong
Southeast University
Peipei Li
The First Affiliated Hospital of Zhengzhou University
Siwei Guo
Shandong University
Fanglei Ye
The First Affiliated Hospital of Zhengzhou University
Jin Jin
Zhejiang University
Renjie Chai
Southeast University

Research Article

Keywords: FAM73a, FAM73b, outer hair cells, macrophage, T cell, IL-12, IFN-γ

Posted Date: September 24th, 2021

DOI: https://doi.org/10.21203/rs.3.rs-883335/v1

Abstract

Mitochondrial dynamics are essential for maintaining the physiological function of the mitochondrial network, and the disorder of mitochondrial dynamics leads to neurodegenerative diseases. However, how mitochondrial dynamics affects auditory function in the inner ear remains unclear. FAM73a and FAM73b are mitochondrial outer membrane proteins that mediate mitochondrial fusion. Here, we found that FAM73a or FAM73b deficiency resulted in elevated oxidative stress and apoptosis of hair cells. Additionally, mitochondrial fission also causes an increase expression of IL-12 in basilar membrane macrophages through accumulating IRF1. As a bridge between innate and adaptive immune responses, hyperproduction of IL-12 further promoted the polarization of Th1 and tissue damage. Our data highlighted an important role of mitochondrial dynamics in maintaining cochlear homeostasis and hair cell survival. Mitochondrial dynamics not only disturbed hair cell function, but also induced the disorder of immune responses.

Introduction

Hearing loss is one of the most common human diseases. According to 2018 World Health Organization report, there are about 466 million people with hearing disability globally, as 5% of the world's total population (https://www.who.int/en/). More than 0.1 percent newborns suffer from hearing loss, which seriously affects a child’s communication, quality of life, and educational attainment[1]. Among all deafness patients, approximately 90% suffer from sensorineural hearing loss (SNHL), which is mainly caused by the loss or damage of cochlear hair cells (HCs) and the degeneration of spiral ganglion neurons after HCs injury.[2] SNHL can be caused by genetic and environmental factors, and genetic defects are responsible for at least 50% of congenital or childhood hearing loss[3]. The identification of the genes associated with hearing loss and their underlying mechanisms remains as an urgent but challenging task.

Mitochondria are essential for the physiological function and survival of HCs, and its dysfunction is involved in the pathogenesis of hearing loss under noise exposure, ototoxic drug treatment, or aging[4]. The disorders of mitochondrial fission and fusion can lead to abnormal morphology and dysfunction, which is implicated in neurodegenerative diseases[5], but the role of mitochondrial dynamics in auditory function has not been extensively investigated. Some evidences have ever shown that dynamin-related protein-1 (Drp-1) is necessary for mitochondrial fission and plays a central role in mitophagy[6, 7]. Reduced Drp-1 expression and mitophagy are involved in age-related hearing loss[8]. Similarly, optic atrophy 1 (OPA1) controls mitochondrial inner membrane fusion, and the R445H mutation in the *Opa1* causes SNHL[9]. Studies have shown that OPA1 is expressed in HCs and spiral ganglion neurons, and its mutation-caused deafness is due to a functional change in the unmyelinated auditory nerve endings and not to a pathological change in HCs[10–12]. FAM73a and FAM73b are mitochondrial outer membrane proteins that are required for mitochondrial outer membrane fusion[13–15]. The deficiency of FAM73a and FAM73b greatly disrupted the mitochondrial morphology, thus it led to higher levels of reactive oxygen

species (ROS) and significant reductions in ATP. However, it remains unclear whether the absence of FAM73a and FAM73b also contribute to deafness similar to Drp-1 and OPA1.

In recent years, immune response and inflammation have also been recognized as one of important pathophysiological factors in HC injury[16]. As a main executor in innate immune system of the cochlea, macrophages are widely distributed in the basilar membrane, the osseous spiral lamina, the lateral wall of the cochlea, and in spiral ganglions under physiological conditions[17]. Adaptive immunity is also considered to be involved in the cochlear immune response[18]. $CD4^+$ T-cells can infiltrate into the basilar membrane and collaborate with macrophages[19]. The resident macrophages of the basilar membrane are activated and produce proinflammatory cytokines, and the monocytes in peripheral circulation also enter the basilar membrane and transform into macrophages in response to noise exposure, ototoxic drug damage, and age-related degeneration[20–23]. In the models of cochlear injury, HC injury is considered to be the initiator of the immune response, and is sufficient to regulate macrophage recruitment into the basilar membrane through fractalkine signaling[24]. The inhibition of the activation and recruitment of macrophages is protective against HC injury caused by ototoxic drugs[25]. FAM73b is involved in macrophage polarization, and regulate the production of IL-12 in response to damage, which further results in increased production of IFN-γ in T cells[26]. Therefore, we investigated the functional changes in macrophages and T cells in the basilar membrane of the cochlea by using *Fam73a* and *Fam73b* knockout (KO) mice, indicated by the expression of inflammatory cytokines and the associated essential signal pathways.

In this study, we found that FAM73a and FAM73b were expressed in the mitochondria of HCs, and *Fam73a* and *Fam73b* KO resulted in HC loss and the destruction of stereocilia structures. Deletion of FAM73a and FAM73b increased the oxidative stress level and apoptosis in HCs. Along with the genetic ablation of FAM73a and FAM73b, the numbers of macrophages and $CD4^+$ T cells in the cochlear basilar membrane were increased, and the expression of the inflammatory cytokines IL-12 and IFN-γ were obviously elevated. After activated by endogenous damage, mitochondrial division in macrophages led to increased expression of Parkin, which degraded the mono-ubiquitinated CHIP protein and stabilized the protein level of downstream transcription factor IRF1, thereby promoting the secretion of IL-12. IL-12 further directly promotes the production of IFN-γ in T cells, which is involved in HC injury. Our data highlighted the role of FAM73a and FAM73b-mediated mitochondrial dynamics in auditory function and clarified the effect of their disorders on HC survival by directly disturbing HC function and indirectly regulating macrophage polarization.

Material And Methods

Mice and genotyping

Genotypic identification of transgenic mice was carried out according to the method described in published literature[26]. All animal experiments were performed in accordance with the protocols approved

by the Animal Care and Use Committee of Southeast University and were consistent with the National Institutes of Health Guide for the Care and Use of Laboratory Animals.

Auditory brainstem response (ABR)

A TDT System III workstation running SigGen32 software (Tucker-Davis Technologies, USA) was used to record ABRs as previously described[27, 28]. The mice were anesthetized by intraperitoneal injection of 0.01 g/ml pentobarbital sodium (100 mg/kg body weight). After deep anesthesia, three fine-needle electrodes were inserted under the skin of the mouse at the vertex of the skull, behind the tested ear, and on the back near the tail. The mice were then put into a soundproof room for the ABR test. The TDT hardware and software (BioSig and SigGen) were used to generate the acoustic signals and to process the responses. The ABRs were elicited with tone bursts at 4, 8, 12, 16, 24, and 32 kHz. The tests were performed at a 5 dB interval from 90 dB to 10 dB at each frequency with a gradually decreasing intensity, and ABR thresholds were recorded as the lowest sound intensity at which a stable wave III could be seen and repeated.

Immunohistochemistry

The basilar membranes of the newborn mouse cochleae were dissected with microsurgery forceps and incubated with 4% paraformaldehyde for 1 h at room temperature (RT), while the basilar membranes from ossified cochleae were carefully dissected with a microsurgery scalpel after incubating in 4% paraformaldehyde and 0.5 M EDTA overnight. Whole mounts of the basilar membrane were then blocked with 10% heat-inactivated donkey serum, 1% bovine serum albumin (BSA), and 1% Triton X-100 in PBS (0.1 M phosphate buffer, pH 7.2) for 1 h at RT. The samples were incubated with primary antibodies diluted in 5% heat-inactivated donkey serum, 1% BSA, and 10% Triton X-100 overnight at 4°C. The tissues were washed three times with PBST (PBS and 1% Triton X-100) and further incubated at RT for 1 h with secondary antibodies (Alexa Fluor 647 or 555 or 488, Invitrogen) diluted in 0.1% BSA and 0.1% Triton X-100. Finally, the tissues were again washed with PBST three times and mounted on a slide. A Zeiss LSM700 confocal microscope was used to take images.

The primary antibodies used in the experiment were FAM73a (Biobyt, orb187931), FAM73b (Novusbio, NBP1-86701), Myosin7a (Proteus Bioscience, 25-6790; DSHB, 138-1); 3-NT (Sigma, N5538), 4-HNE (Abcam, ab46545), F4/80 (Abcam, ab6640); Iba1 (Wako Pure Chemicals, 019-19741), IL-12 (Abcam, ab210255), MHCII (Abcam, ab23990), CD4 (Santa Cruz Biotechnology, sc-20079), IRF1 (Santa Cruz Biotechnology, sc-514544), and Parkin (Santa Cruz Biotechnology, sc-32282). A TUNEL kit (Vazyme, A112-03) was used to detect apoptotic cells according to the manufacturer's instructions.

qRT-PCR

Total RNA from the brain, from different parts of the cochlea, and from whole cochleae was extracted with ExTrizol Reagent (Protein Biotechnology, PR910), and the reverse transcription from mRNA to cDNA was carried out using cDNA Synthesis kits (Thermo Fisher Scientific, K1622) according to the

manufacturer's instructions. The qPCR was performed using an Applied Biosystems CFX96 qPCR system (Bio-Rad, Hercules, CA, USA) and the SYBR Green (Rox) qPCR Master Mix (Roche Life Science, 04913850001). Validated primers were designed for targeted DNA or mRNA sequences (Table1). The qPCR protocol was an initial denaturing step of 15 s at 95°C followed by 40 cycles of 15 s denaturation at 95°C, 60 s annealing at 60°C, and 20 s extension at 72°C. The expression of mRNA was normalized using the values of *Gapdh*, and the results were analyzed using the comparative cycle threshold (ΔΔCt) method.

Western blot

Cochleae from two mice were dissected in cold PBS and lysed with 150 ml RIPA Lysis Buffer (Medium, Hangzhou Fu De Biological Technology) and 3 μl 50× protease inhibitor cocktail (Hangzhou Fu De Biological Technology) at 4°C. The primary antibodies were detected by HRP-conjugated secondary antibodies using the ECL detection system. The western blot bands were semiquantified using ImageJ software, and the band densities were normalized to background and the relative optical density ratio was calculated by comparison to the reference protein GAPDH or β-actin.

Each experiment was repeated at least three times. The following primary antibodies were used: FAM73a (Abcam, ab121532), FAM73b (Santa Cruz Biotechnology, sc-20437), 3-NT (Sigma, N5538), Arg1 (Abcam, ab239731), IRF1 (Santa Cruz Biotechnology, sc-514544), Parkin (Santa Cruz Biotechnology, sc-32282), CHIP (Santa Cruz Biotechnology, sc-133066), and ubiquitin (Santa Cruz Biotechnology, sc-8017).

Immunoprecipitation (IP)

Cochleae from two mice were lysed with 150 ml RIPA lysis buffer (Medium, Hangzhou Fu De Biological Technology). CHIP was isolated with antibodies targeting CHIP (Santa Cruz Biotechnology, sc-133066), and Protein A+G was used to capture the antibodies. The ubiquitinated proteins were detected by western blot using anti-ubiquitin antibodies (Santa Cruz Biotechnology, sc-8017).

Scanning electron microscopy

The cochlear specimens from P30 mice were collected and immediately fixed in 2.5% glutaraldehyde (Sigma-Aldrich, G5882) diluted in 0.1 M phosphate buffer (pH 7.2) for 24 h at 4°C. The tissues were then decalcified for 3 h in 0.5 M EDTA, post-fixed for 2 h at 4°C in 1% osmium tetroxide, dehydrated in ethanol, and embedded in araldite CY 212 (TAAB, E009). The ultrathin sections were stained with alcoholic uranyl acetate (Polysciences, 6159–44–0) and alkaline lead citrate (SigmaAldrich, 15326), washed gently with distilled water, and imaged with a JEM 1230 transmission electron microscope (JEOL Ltd, Tokyo, Japan).

Fluorescence intensity measurement

Different groups of cochleae were fixed, labeled with the same solution, and processed in parallel. The tissue was photographed with confocal microscope using the same parameters. The immunolabeling

intensity of antibodies was measured using ImageJ software in which a region of interest was drawn and the mean gray value intensities were measured from 4 or 5 sections per cochlea.

The number and morphology of basilar membrane macrophages

Macrophages were distributed throughout the basilar membrane, and exhibited dendritic, irregular, amoeboid, and spherical morphology. They were identified with surface markers F4/80 and Iba1 as have been used in previous studies[29]. To assess the number of macrophages in the apical, middle, and basal turns of the basilar membrane, F4/80-labeled macrophages were counted under the confocal microscope. Images at 20× magnification taken from each turn of the cochlear whole mounts were used as representative figures. To measure the size of macrophages, ImageJ software was used to outline the membrane boundaries of each cell and calculated the area contained in the drawn region. Five typical cells were selected from each turn of tissue specimen, and their average area represented the size of apical, middle, and basal turns macrophages in the basilar membrane of each individual cochlea.

Macrophage phagocytosis

PHrodo® zymosan bioparticles conjugate (Invitrogen, P35365) was used to evaluate the phagocytic activity of macrophages. The fluorescence of the pHrodo® dye was activated when the zymosan bioparticles were ingested and exposed to a more acidic PH within the acidic phagocytic vacuoles. Because the extracellular pH is more alkaline, bioparticle fluorescence was absent outside the cell. The cochleae were dissected from the skull and placed in live cell imaging solution (A14291DJ, Invitrogen). The membrane labyrinth was opened from the top of the cochlea to remove the basilar membrane, modiolus, and the lateral wall tissue, thereby exposing the inner surface of lateral wall of scala tympani at the basal turn of the cochlea. Then the basal turn was divided into several pieces so that the cochlear bone wall could be flat on the slide. PHrodo® zymosan bioparticles® conjugate incubated the collected tissues for 90 minutes at 37°C, and then they were rinsed three times for 5 min each using live cell imaging solution. 4% buffered formalin fixed the collected tissues for 4 hours and then EDTA decalcified at 4°C for 1 day. Subsequently, the primary antibody against F4/80 and the appropriate secondary antibody incubated the collected tissues to visualize macrophages.

Drug administration

Clophosome®-A - Clodronate Liposomes (LCCA) (FormuMax, F70101C-A) provide superior efficiency of macrophage depletion. We intraperitoneally injected mice with LCCA every other day from P30 to P60 at 70 mg/kg. We collected and dissected the cochleae and measured HC loss and the number of macrophages when the drug administration was completed.

Statistical analysis

Microsoft Excel and GraphPad Prism software were used for statistical analyses. All of the data are presented as mean ± SD, and all experiments were repeated at least three times. Two-tailed, unpaired

Student's t-tests were performed. P-values <0.05 were considered significant, and the level of significance is indicated as *P < 0.05, **P < 0.01, ***P < 0.001. All statistical tests were justified as appropriate, and the data met the assumptions of the tests. The variance was similar between the statistically compared groups.

Results

FAM73a and FAM73b are expressed in cochlea

To determine whether FAM73a and FAM73b are expressed in the cochlea, qRT-PCR was performed in the brain and cochlear tissue of postnatal day 3 (P3) WT mice. *Fam73a* and *Fam73b* were indeed expressed in the basilar membrane, lateral wall, and modiolus of the cochlea, although their expression in these regions are not as high as that in brain tissue (Fig. 1A,D). To study their expression pattern during postnatal development, we further examined the expression of *Fam73a* and *Fam73b* by qRT-PCR in different age groups. The levels of *Fam73a* and *Fam73b* decreased from P14 but was still presented in P30 mice (Fig. 1B,E). Western blots also verified the proteins levels of FAM73a and FAM73b in the cochleae of P14 and P30 WT mice (Fig. 1C,F). We then immunolabeled FAM73a and FAM73b with Myosin7a in the whole-mount basilar membrane. Confocal imaging at P3 revealed that FAM73a and FAM73b were expressed in the cytoplasm of HCs rather than in the nucleus (Fig. 1G-H). In P14 and P30 WT mice, FAM73a and FAM73b were stably expressed in the cytoplasm of HCs (Fig. 1I-J). These results suggest FAM73a and FAM73b were expressed in the cochlea at all stages of development.

FAM73a and FAM73b KO mice show progressive hearing loss

To evaluate whether FAM73a and FAM73b affect auditory function and HC survival, we constructed *Fam73a* and *Fam73b* KO mice. We first confirm the efficiency of FAM73a and FAM73b deletion in the cochlea in P30 KO mice by qRT-PCR (Supplementary Fig. 1A,C) and immunolabeling (Supplementary Fig. 1B,D). We then evaluated the hearing levels in these mice using the ABR test. In P30 KO mice, ABR thresholds were significantly increased at middle and high frequencies after *Fam73a* deletion, while *Fam73b* deficiency led to elevated ABR thresholds at all frequencies (Fig. 2A,G). A similar high-frequency hearing loss was observed both in these two KO mice, but *Fam73b* deletion caused an earlier and more severe hearing loss at low and middle frequencies than those in *Fam73a* deletion. Although inner HC loss was not observed, outer hair cell (OHC) loss was consistent with the trend of hearing loss. Scattered OHC loss was seen in the apical, middle, and basal turns both in these two KO mice, and the most severe damage was found in the basal turn (Fig. 2B,C,H,I). However, *Fam73a* KO mice showed no significant difference of OHC loss in the apical turn (Fig. 2B,C). In P60 KO mice, the absence of FAM73a and FAM73b resulted in severe hearing loss (Fig. 2D,J), and the OHC loss in each turn was more severe than that of P30 KO mice (Fig. 2E,F,K,L). We also observed the ultrastructure of the stereocilia in P30 KO mice with a scanning electron microscope and found that the knockout of *Fam73a* and *Fam73b* led to the degeneration of the stereocilia (Fig. 2M,N). It was noteworthy that the OHC loss caused by FAM73b

deficiency was stronger than that of FAM73a deficiency, and the degree of OHC loss and hearing loss at P60 were worse than those at P30.

Lack of FAM73a and FAM73b causes apoptosis of HCs by enhancing oxidative stress

Previous evidences revealed that absence of *Fam7a* and *Fam73b* results in elevated level of oxidative stress[13]. To clarify how FAM73a and FAM73b cause injury on HCs, we thus evaluated the changes of mitochondrial ROS in the HCs of *Fam73a* and *Fam73b* KO mice by detecting the oxidative stress markers 3-nitrotyrosine (3-NT) and 4-hydroxynonenal (4-HNE) . In P21 mice, confocal images showed that the levels of 3-NT and 4-HNE were already increased in *Fam73a* or *Fam73b* KO mice (Fig. 3A,C,E,G). Quantification of the immunofluorescence intensity confirmed a significant increase in these two KO mice compared to WT control (Fig. 3B,D,F,H). Western blots also showed increased expression of 3-NT both in *Fam73a* and *Fam73b* KO mice compared to controls (Fig. 3I,J). As known, increased oxidative stress can activate apoptosis signaling pathways and induce cell death, so we performed TUNEL staining to identify apoptotic HCs in P21 *Fam73a* and *Fam73b* KO mice. Immunofluorescence staining showed that TUNEL-positive cells were found in these two KO mice but not in WT mice (Fig. 4A,B,D,E). The qRT-PCR results showed that the expressions of proapoptotic marker genes, including *Bax*, *Casp3*, *Casp8*, *Casp9*, and *Apaf1* was significantly higher in the KO mice than those in WT mice (Fig. 4C,F). These results indicate that lack of FAM73a or FAM73b increases oxidative stress in HCs, and subsequent high ROS levels cause apoptosis in HCs.

FAM73a and FAM73b deficiency provokes innate and adaptive immune responses in the basilar membrane

Previous studies have shown that macrophages and $CD4^+$ T cells are recruited into the basilar membrane of the cochlea after HC damage[19, 24]. FAM73b deficiency has been reported to be essential for the polarization of type 1 macrophages under Toll-like receptor stimulation by controlling mitochondrial morphology switching from fusion to fission[26]. Therefore, we investigate whether *Fam73a* and *Fam73b* in immune cells are also involved in the development of deafness. We measured the infiltration of macrophages and $CD4^+$ T cells in the basilar membrane in *Fam73a* and *Fam73b* KO mice. Strikingly, the numbers of macrophages in the basilar membrane were increased in P30 *Fam73a* and *Fam73b* KO mice compared to WT control (Fig. 5A,B,E,F). In P60 KO mice, the numbers of macrophages were significantly increased in the apical, middle, and basal turns (Fig.5 C,D,G,H). In P30 WT mice, resident macrophages exhibited a slender body with multiple length dendritic projections. Macrophage in *Fam73a* KO mice showed a similar morphology (Fig. 5A), but their bodies were enlarged in the *Fam73b* KO mice (Fig. 5E). In P60 WT mice, the macrophage bodies were larger than those in P30 mice in the middle and basal turns (Fig. 5C,G). *Fam73a* KO mice also exhibited a similar phenotype of macrophage morphology. In the *Fam73b* KO mice, most of the macrophages transformed into giant irregular or spherical shapes (Fig. 5C,G). The quantitative results confirmed our above observations that the average size of the macrophages in both KO mice was significantly larger than in WT mice (Fig. 5J,M), suggesting an activating morphological transformation in these two KO mice. This difference in morphologic

transformation between the two KO mice might be due to the different degree of HC damage, because *Fam73b* KO mice showed earlier and more severe HC damage. Furthermore, we also found that the number of $CD4^+$ T cells in P45 KO mice was significantly increased in the whole length of the basilar membrane compared to WT mice (Fig. 5I,K,L,N), indicating an adaptive immune response occurred in two KO mice lines. These results support the hypothesis that lack of FAM73a and FAM73b provokes innate and adaptive immune responses in the basilar membrane.

Lack of FAM73a and FAM73b promotes the expressions of IL-12 and IFN-γ in basilar mebrane.

Because macrophage is a resident immune cell of the basilar membrane , it can affect pathological changes in HC. The phagocytic activity of macrophages is involved in the removal of unwanted or damaged cochlear tissues under both normal and pathological conditions. We thus examine whether phagocytic function of *Fam73a* and *Fam73b* KO macrophages distributed on the lateral wall of the scala tympani at the basal turn changed using a confocal microscope (Fig. 6A-H). Although no significant difference in number of macrophages were found between the WT and *Fam73a* KO mice (Fig.6B), that in *Fam73b* KO mice was significantly decreased (Fig.6F), implying that more macrophages are recruited into the basilar membrane due to a severe HC damage in *Fam73b* KO mice. However, phagocytic activity of these macrophages displayed no difference compared to WT control, suggested by a similar fluorescence uptaking using pHrodo® fluorescent bioparticles (Fig.6C,G). The quantitative results confirmed these observations (Fig.6D,H). Collectively, these findings demonstrated that FAM73a and FAM73b deficiency did not regulate the phagocytic capacity of cochlear macrophages.

Because the different recruitment of macrophages and T cells were observed between KO and WT mice, we further evaluated whether FAM73a and FAM73b deficiency triggered cochlear inflammatory activity. We examined the transcriptional levels of proinflammatory cytokines (*Il12a, Il12b, Ifng, Il6, Il1b*, and *Tnfa*), and anti-inflammatory activity (*Il10*) in the cochlea by qRT-PCR. In P60 *Fam73a* KO or *Fam73b* KO mice, the mRNA levels of *Il12a* and *Ifng* were significantly increased both in *Fam73a* and *Fam73b* KO mice compared with WT group (Fig. 7A), while *Il10* was significantly decreased (Fig. 7D). No difference in mRNA levels of *Il6* and *Il1b* was observed, suggesting *Fam73a* and *Fam73b* deficiency only induced a partial phenotypes of M1 subtype. Consistently, M2-type macrophage marker *Cd206* and *Arg1* was significantly decreased in P60 *Fam73a* or *Fam73b* KO mice compared with WT mice (Fig. 7B, 7E). The western blot analysis confirmed the downregulation of ARG1 protein expression both in these two KO mice (Fig. 7C,F). To further verify the enhanced expression of IL-12, we immunolabeled IL-12 in the macrophages of the basilar membrane. We found that the expression of IL-12 in macrophages was upregulated in these two P60 KO mice (Fig. 7G-J). To determine whether the antigen presentation function of macrophages was enhanced by the increased expression of IL-12, we immunolabeled MHCII – an antigen-presenting protein – in macrophages. Interestingly, we also found that the expression of MHCII in *Fam73a* or *Fam73b* KO macrophages was increased compared with WT mice (Fig. 7K-N). These findings suggest that mitochondrial dynamics regulates IL-12 expression and capacity of antigen presentation in macrophages, which further promotes the expression of IFN-γ in $CD4^+$ T cells.

To prove the role of macrophages in HC damage in the cochlea, LCCA was intraperitoneally injected into KO mice to deplete macrophages from P30 to P60. We found that the numbers of macrophages were significantly decreased in the basilar membrane of P60 KO mice after LCCA injection (Fig. 8A-B,E-F). After deletion of macrophages by LCCA, HC loss was obviously reduced in P60 *Fam73a* and *Fam73b* KO mice compared to the untreated groups (Fig. 8C-D,G-H). These results suggest macrophages play an important role in HC injury in *Fam73a* and *Fam73b* KO mice.

FAM73a and FAM73b control macrophage function via regulating Parkin-CHIP-IRF1 signaling

A previous study reported that mitochondrial fission caused by *Fam73b* ablation increases the expression of Parkin and IRF1, which further promoting the production of IL-12[26]. To determine the role of Parkin-IRF1 signal in the cochlea of *Fam73a* and *Fam73b* KO mice, we first performed qRT-PCR to determine the mRNA level of *Irf1*. The expression of *Irf1* was not significantly different in P60 *Fam73a* or *Fam73b* KO mice compared with WT control (Fig. 9A,D). However, western blots showed a significantly upregulated expression of IRF1 in the cochlea of these two KO mice (Fig. 9B-C,E-F). To further verify the increased expression of IRF1 in macrophages in the basilar membrane, we co-stained IRF1 and Iba1 in the whole mount tissue. Confocal images showed an obviously enhanced expression of IRF1 in KO macrophages compared with WT littermate (Fig. 9G-H,I-J). Monoubiquitinated CHIP promoted the degradation of IRF-1, thus we also found the protein expression level of mono-ubiquitinated CHIP was significantly reduced in P60 *Fam73a* or *Fam73b* KO mice compared with WT mice (Fig. 10A-D). Lastly, qRT-PCR assay (Fig. 11A,D) and western blots (Fig. 11B-C,E-F) showed that mRNA and protein levels of *Park2* was significantly upregulated in P60 these two KO mice. To further confirm that the expression of Parkin was upregulated in macrophages of basilar membrane, we immunolabeled Parkin and Iba1 in macrophages. The increased expression of Parkin was observed by confocal images of macrophages from KO mice (Fig. 11G-H,I-J). Together these results suggest a similar regulating mechanism between peripheral macrophages and those in the cochlea via Parkin-CHP-IRF1 signal to control the production of IL-12.

Discussion

Mitochondria provide energy for cellular activity and thus play key roles in cell survival, apoptosis, and metabolism. Mitochondrial morphology switching between fusion and fission affects mitochondrial function and leads to changes in the production of ROS and mitophagy. Previous studies have shown that increased levels of ROS damage HCs in noise-, drug- and age-related hearing loss[30–32]. The mitophagy protects against HC injury caused by noise exposure, ototoxic drug treatment, and age-related degeneration[8, 33, 34]. However, the roles of mitochondrial membrane proteins regulating mitochondrial morphology, including Mitofusin 1 (MFN1) and MFN2, in HCs remains unclear due to embryonic lethality of deficient mice. OPA1, as a protein of regulating mitochondrial inner membrane fusion, causes SHNL through auditory neuropathy but not HC injury. Recent studies showed that *Fam73a* and *Fam73b* KO mice are viable and can be used as a suitable model to study the influence of mitochondrial dynamics on auditory function in the inner ear. Our results indicate that FAM73a and FAM73b deficiency results in HC damage through increased production of ROS and the destruction of stereocilia structures. These results

suggest that the absence of FAM73a and FAM73b has a harmful effect on HCs through oxidative stress rather than a protective effect through mitophagy.

Previous studies have shown that HC injury increases the number of macrophages and transforms macrophage morphology into an activated shape[24, 25]. Our study shows that the number of macrophages significantly increases accompanied by larger in size when HCs are severely damaged. To further explore the role of macrophages in HC death, we examined the phagocytic capacity of macrophages. However, the phagocytic capacity of macrophages localized at the luminal surface of the scale tympani cavity did not change in *Fam73a* and *Fam73b* KO mice compared with the controls. Intraperitoneal injection of LCCA not only deplete macrophages, but also significantly reduced HC damage. Therefore, we believe that macrophages play a detrimental role in HC injury. These results indicate that HC injury activates macrophages by releasing certain endogenous factors triggering the cochlear immune response, and the next studies should identify these molecules and clarify their inducible mechanism.

The activation of macrophage trigger the production of multiple inflammatory cytokines such as TNF-α, IL-1β, IL-6, and CCL2 under noise exposure, ototoxic drug treatment, and age-related degeneration[35–38]. However, there is no report on the expression of IL-12 and IFN-γ in these models with cochlear aseptic inflammation. Clinical studies have found that TNF-α might play critical roles in sudden SNHL based on blood samples from patients, while IL-12, IFN-γ and IL-10 have been shown not to participate in the pathophysiology of sudden SNHL [39, 40]. We found that the expression of proinflammatory cytokines IL-12 and IFN-γ increased, while the anti-inflammatory cytokine IL-10 decreased in *Fam73a* and *Fam73b* KO mice, and this suggests a novel mechanism of inflammation in SNHL occurrence caused by the disorder of mitochondrial morphology.

Previous studies have shown that the production of inflammatory cytokines in the cochlea is attributed to the activation of toll-like receptors on the surface of macrophages[41] under noise exposure or ototoxic drug treatment. TLR4 promotes the production of ROS and the activation of the downstream NF-kB signaling pathway[42–44]. However, our results presented a novel signal pathway which is composed by Parkin–CHIP–IRF1[26]. This signal pathway regulated the production of IL-12 in macrophages is independent of ROS or NF-kB, which is different from previous studies. Our data show that the expression of IRF1 and Parkin in macrophages is increased, while the level of monoubiquitinated CHIP is decreased. These results indicate that macrophages modulate the production of inflammatory cytokines through a novel signal pathway in the cochlea of *Fam73a* and *Fam73b* KO mice.

Although macrophages representing innate immune responses have been well studied in the cochlea, the role of adaptive immune responses remains unclear. Adaptive immune cells have been shown to be involved in noise-induced cochlear damage[18]. $CD4^+$ T cells exist in the modiolus of the cochlea under physiological conditions and can enter the basilar membrane of the cochlea together with macrophages in response to noise-induced damage[19, 45]. Additionally, inhibition of nuclear factor of activated T cells

(NFAT) protects HCs against aminoglycoside ototoxicity[46]. Although these studies have shown the presence of T cells in the inner ear and their activation can damage HCs, its underlying mechanism affecting HC injury remains unknown. Our results showed that the number of $CD4^+$ T cells in the basilar membrane and the expression of IFN-γ derived from $CD4^+$ T cells is significantly elevated in the cochlea of *Fam73a* and *Fam73b* KO mice. These results implies that $CD4^+$ T cells induced the damage of HCs by secreting IFN-γ, which is the first time to report the T cell-mediated mechanism in HCs damage.

In conclusion, our study provides disrupted mitochondrial morphology switching as a new risk factor for SNHL. FAM73a and FAM73b are essential for the survival of HCs and the maintenance of auditory function. The deletion of FAM73a and FAM73b induces innate and adaptive immune responses in the cochlea. IL-12 and IFN-γ, expressing in macrophages and T cells respectively, are involved in the development of SNHL caused by mitochondrial fission. Our data also demonstrated a new Parkin-CHIP-IRF1 signaling pathway that regulates the production of inflammatory cytokines in macrophages after cochlear injury. Our findings suggest a new mechanism of SNHL and provide a new direction for the clinical prevention and therapeutic treatment of SNHL.

Declarations

Funding Information

This work was supported by grants from National Key R&D Program of China (No. SQ2020YFA010013), the Strategic Priority Research Program of the Chinese Academy of Science (XDA16010303), the National Key R&D Program of China (Nos. 2017YFA0103903 and 2018YFA0800503), the National Natural Science Foundation of China (Nos. 82071046, 82030029, 81970882 and 81771675), the Natural Science Foundation from Jiangsu Province (BE2019711), the Shenzhen Fundamental Research Program (JCYJ20190814093401920), Boehringer Ingelheim Pharma GmbH, and the Open Research Fund of State Key Laboratory of Genetic Engineering, Fudan University (No. SKLGE-2104).

Compliance with Ethical Standards

We performed all animal procedures according to protocols that were approved by the

Animal Care and Use Committee of Southeast University and that were consistent with the National Institute of Health's Guide for the Care and Use of Laboratory Animals.We made all efforts to minimize the number of animals used and to prevent their suffering.

Authors' Contributions

Renjie Chai, Fanglei Ye and Jin Jin designed and supervised the project. Yuan Zhang, Xiaolong Fu, Yiyuan Li, Guodong Hong, Peipei Li and Siwei Guo performed most experiments and acquired the data. Yuan Zhang, Xiaolong Fu, Yiyuan Li, Guodong Hong, Peipei Li and Siwei Guo analyzed and interpreted the experiments results. Yuan Zhang, Xiaolong Fu and Renjie Chai wrote the manuscript.

Conflict of Interest

The authors declare no competing interests.

Availability of Data and Material

The data that support the findings of this study are available from the corresponding author upon reasonable request.

References

1. McDermott JH, Molina-Ramirez LP, Bruce IA, Mahaveer A, Turner M, Miele G, Body R, Mahood R, Ulph F, MacLeod R, Harvey K, Booth N, Demain LAM, Wilson P, Black GC, Morton CC (2019) W. G. Newman, Diagnosing and Preventing Hearing Loss in the Genomic Age. Trends Hear 23:2331216519878983
2. Marler JA, Elfenbein JL, Ryals BM, Urban Z, Netzloff ML (2005) Sensorineural Hearing Loss in Children and Adults with Williams Syndrome. Am J Med Genet A 138(4):318–327
3. Yang T, Guo L, Wang L, Yu X (2019) Diagnosis, Intervention, and Prevention of Genetic Hearing Loss. Adv Exp Med Biol 1130:73–92
4. Bottger EC, Schacht J (2013) The Mitochondrion: A Perpetrator of Acquired Hearing Loss. Hear Res 303:12–19
5. Burte F, Carelli V, Chinnery PF, Yu-Wai-Man P (2015) Disturbed Mitochondrial Dynamics and Neurodegenerative Disorders. Nat Rev Neurol 11(1):11–24
6. Youle RJ, van der Bliek AM (2012) Mitochondrial Fission, Fusion, and Stress. Science 337(6098):1062–1065
7. Feng ST, Wang ZZ, Yuan YH, Wang XL, Sun HM, Chen NH, Zhang Y (2020) Dynamin-Related Protein 1: A Protein Critical for Mitochondrial Fission, Mitophagy, and Neuronal Death in Parkinson's Disease. Pharmacol Res 151:104553
8. Lin H, Xiong H, Su Z, Pang J, Lai L, Zhang H, Jian B, Zhang W, Zheng Y (2019) Inhibition of Drp-1-Dependent Mitophagy Promotes Cochlea Hair Cell Senescence and Exacerbates Age-Related Hearing Loss. Front Cell Neurosci 13:550
9. Amati-Bonneau P, Odent S, Derrien C, Pasquier L, Malthiery Y, Reynier P, Bonneau D (2003) The Association of Autosomal Dominant Optic Atrophy and Moderate Deafness May Be Due to the R445h Mutation in the Opa1 Gene. Am J Ophthalmol 136(6):1170–1171
10. Bette S, Zimmermann U, Wissinger B, Knipper M (2007) Opa1, the Disease Gene for Optic Atrophy Type Kjer, Is Expressed in the Inner Ear. Histochem Cell Biol 128(5):421–430
11. Huang T, Santarelli R, Starr A (2009) Mutation of Opa1 Gene Causes Deafness by Affecting Function of Auditory Nerve Terminals. Brain Res 1300:97–104
12. Rosamaria Santarelli R, Rossi P, Scimemi E, Cama ML, Valentino CL, Morgia L, Caporali R, Liguori V, Magnavita A, Monteleone (2015) Ariella Biscaro, Edoardo Arslan, Valerio Carelli, Opa1-Related

Auditory Neuropathy, 138. Site of Lesion and Outcome of Cochlear Implantation, Brain, pp 563–576

13. Zhang Y, Liu X, Bai J, Tian X, Zhao X, Liu W, Duan X, Shang W, Fan HY, Tong C (2016) Mitoguardin Regulates Mitochondrial Fusion through Mitopld and Is Required for Neuronal Homeostasis. Mol Cell 61(1):111–124
14. Liu XM, Zhang YP, Ji SY, Li BT, Tian X, Li D, Tong C, Fan HY, Mitoguardin-1 and – 2 Promote Maturation and the Developmental Potential of Mouse Oocytes by Maintaining Mitochondrial Dynamics and Functions, Oncotarget, 2016, 7(2): 1155-67
15. Liu XM, Zhang YL, Ji SY, Zhao LW, Shang WN, Li D, Chen Z, Tong C, Fan HY, Mitochondrial Function Regulated by Mitoguardin-1/2 Is Crucial for Ovarian Endocrine Functions and Ovulation, Endocrinology, 2017, 158(11): 3988–3999
16. Wood MB, Zuo J (2017) The Contribution of Immune Infiltrates to Ototoxicity and Cochlear Hair Cell Loss. Front Cell Neurosci 11:106
17. Hu BH, Zhang C, Frye MD (2018) Immune Cells and Non-Immune Cells with Immune Function in Mammalian Cochleae. Hear Res 362:14–24
18. Rai V, Wood MB, Feng H, Schabla NM, Tu S, Zuo J (2020) The Immune Response after Noise Damage in the Cochlea Is Characterized by a Heterogeneous Mix of Adaptive and Innate Immune Cells. Sci Rep 10(1):15167
19. Yang W, Vethanayagam RR, Dong Y, Cai Q, Hu BH, Activation of the Antigen Presentation Function of Mononuclear Phagocyte Populations Associated with the Basilar Membrane of the Cochlea after Acoustic Overstimulation, Neuroscience, 2015, 303: 1–15
20. Kaur T, Ohlemiller KK, Warchol ME (2018) Genetic Disruption of Fractalkine Signaling Leads to Enhanced Loss of Cochlear Afferents Following Ototoxic or Acoustic Injury. J Comp Neurol 526(5):824–835
21. Frye MD, Zhang C, Hu BH (2018) Lower Level Noise Exposure That Produces Only Tts Modulates the Immune Homeostasis of Cochlear Macrophages. J Neuroimmunol 323:152–166
22. Frye MD, Yang W, Zhang C, Xiong B, Hu BH (2017) Dynamic Activation of Basilar Membrane Macrophages in Response to Chronic Sensory Cell Degeneration in Aging Mouse Cochleae. Hear Res 344:125–134
23. Dhukhwa A, Bhatta P, Sheth S, Korrapati K, Tieu C, Mamillapalli C, Ramkumar V, Mukherjea D (2019) Targeting Inflammatory Processes Mediated by Trpvi and Tnf-Alpha for Treating Noise-Induced Hearing Loss. Front Cell Neurosci 13:444
24. Kaur T, Zamani D, Tong L, Rubel EW, Ohlemiller KK, Hirose K, Warchol ME (2015) Fractalkine Signaling Regulates Macrophage Recruitment into the Cochlea and Promotes the Survival of Spiral Ganglion Neurons after Selective Hair Cell Lesion. J Neurosci 35(45):15050–15061
25. Sun S, Yu H, Yu H, Honglin M, Ni W, Zhang Y, Guo L, He Y, Xue Z, Ni Y, Li J, Feng Y, Chen Y, Shao R, Chai R, Li H (2015) Inhibition of the Activation and Recruitment of Microglia-Like Cells Protects against Neomycin-Induced Ototoxicity. Mol Neurobiol 51(1):252–267

26. Gao Z, Li Y, Wang F, Huang T, Fan K, Zhang Y, Zhong J, Cao Q, Chao T, Jia J, Yang S, Zhang L, Xiao Y, Zhou JY, Feng XH, Jin J (2017) Mitochondrial Dynamics Controls Anti-Tumour Innate Immunity by Regulating Chip-Irf1 Axis Stability. Nat Commun 8(1):1805
27. Zhu C, Cheng C, Wang Y, Muhammad W, Liu S, Zhu W, Shao B, Zhang Z, Yan X, He Q, Xu Z, Yu C, Qian X, Lu L, Zhang S, Zhang Y, Xiong W, Gao X, Xu Z, Chai R (2018) Loss of Arhgef6 Causes Hair Cell Stereocilia Deficits and Hearing Loss in Mice. Front Mol Neurosci 11:362
28. Fang Q, Zhang Y, Da P, Shao B, Pan H, He Z, Cheng C, Li D, Guo J, Wu X, Guan M, Liao M, Zhang Y, Sha S, Zhou Z, Wang J, Wang T, Su K, Chai R, Chen F (2019) Deletion of Limk1 and Limk2 in Mice Does Not Alter Cochlear Development or Auditory Function. Sci Rep 9(1):3357
29. Okano T, Nakagawa T, Kita T, Kada S, Yoshimoto M, Nakahata T, Ito J (2008) Bone Marrow-Derived Cells Expressing Iba1 Are Constitutively Present as Resident Tissue Macrophages in the Mouse Cochlea. J Neurosci Res 86(8):1758–1767
30. Sun HY, Hu YJ, Zhao XY, Zhong Y, Zeng LL, Chen XB, Yuan J, Wu J, Sun Y, Kong W, Kong WJ (2015) Age-Related Changes in Mitochondrial Antioxidant Enzyme Trx2 and Txnip-Trx2-Ask1 Signal Pathways in the Auditory Cortex of a Mimetic Aging Rat Model: Changes to Trx2 in the Auditory Cortex. FEBS J 282(14):2758–2774
31. Wu F, Xiong H, Sha S (2020) Noise-Induced Loss of Sensory Hair Cells Is Mediated by Ros/Ampkalpha Pathway. Redox Biol 29:101406
32. Han H, Dong Y, Ma X (2020) Dihydromyricetin Protects against Gentamicin-Induced Ototoxicity Via Pgc-1alpha/Sirt3 Signaling in Vitro. Front Cell Dev Biol 8:702
33. He Z, Guo L, Shu Y, Fang Q, Zhou H, Liu Y, Liu D, Lu L, Zhang X, Ding X, Liu D, Tang M, Kong W, Sha S, Li H, Gao X, Chai R, Autophagy Protects Auditory Hair Cells against Neomycin-Induced Damage, Autophagy, 2017, 13(11): 1884–1904
34. Yuan H, Wang X, Hill K, Chen J, Lemasters J, Yang SM, Sha SH (2015) Autophagy Attenuates Noise-Induced Hearing Loss by Reducing Oxidative Stress. Antioxid Redox Signal 22(15):1308–1324
35. He W, Yu J, Sun Y, Kong W (2020) Macrophages in Noise-Exposed Cochlea: Changes, Regulation and the Potential Role. Aging disease 11(1):191–199
36. Frye MD, Ryan AF, Kurabi A (2019) Inflammation Associated with Noise-Induced Hearing Loss. J Acoust Soc Am 146(5):4020
37. Watson N, Ding B, Zhu X, Frisina RD (2017) Chronic Inflammation - Inflammaging - in the Ageing Cochlea: A Novel Target for Future Presbycusis Therapy. Ageing Res Rev 40:142–148
38. Kalinec GM, Lomberk G, Urrutia RA, Kalinec F (2017) Resolution of Cochlear Inflammation: Novel Target for Preventing or Ameliorating Drug-, Noise- and Age-Related Hearing Loss. Front Cell Neurosci 11:192
39. Demirhan E, Eskut NP, Zorlu Y, Cukurova I, Tuna G, Kirkali FG (2013) Blood Levels of Tnf-Alpha, Il-10, and Il-12 in Idiopathic Sudden Sensorineural Hearing Loss. Laryngoscope 123(7):1778–1781
40. Yoon SH, Kim ME, Kim HY, Lee JS, Jang CH (2019) Inflammatory Cytokines and Mononuclear Cells in Sudden Sensorineural Hearing Loss. J Laryngol Otol 133(2):95–101

41. Vethanayagam RR, Yang W, Dong Y, Hu BH (2016) Toll-Like Receptor 4 Modulates the Cochlear Immune Response to Acoustic Injury. Cell Death Dis 7(6):e2245
42. Zhang G, Zheng H, Pyykko I, Zou J (2019) The Tlr-4/Nf-Kappab Signaling Pathway Activation in Cochlear Inflammation of Rats with Noise-Induced Hearing Loss. Hear Res 379:59–68
43. So H, Kim H, Lee JH, Park C, Kim Y, Kim E, Kim JK, Yun KJ, Lee KM, Lee HY, Moon SK, Lim DJ, Park R (2007) Cisplatin Cytotoxicity of Auditory Cells Requires Secretions of Proinflammatory Cytokines Via Activation of Erk and Nf-Kappab. J Assoc Res Otolaryngol 8(3):338–355
44. Oh GS, Kim HJ, Choi JH, Shen A, Kim CH, Kim SJ, Shin SR, Hong SH, Kim Y, Park C, Lee SJ, Akira S, Park R (2011) H. S. So, Activation of Lipopolysaccharide-Tlr4 Signaling Accelerates the Ototoxic Potential of Cisplatin in Mice. J Immunol 186(2):1140–1150
45. Liu W, Rask-Andersen H (2019) Super-Resolution Immunohistochemistry Study on Cd4 and Cd8 Cells and the Relation to Macrophages in Human Cochlea. J Otol 14(1):1–5
46. Sekulic-Jablanovic M, Voronkova K, Bodmer D, Petkovic V, Combination of Antioxidants and Nfat (Nuclear Factor of Activated T Cells) Inhibitor Protects Auditory Hair Cells from Ototoxic Insult, J. Neurochem., 2020: 11

Table

Due to technical limitations, table 1 is only available as a download in the Supplemental Files section.

Figures

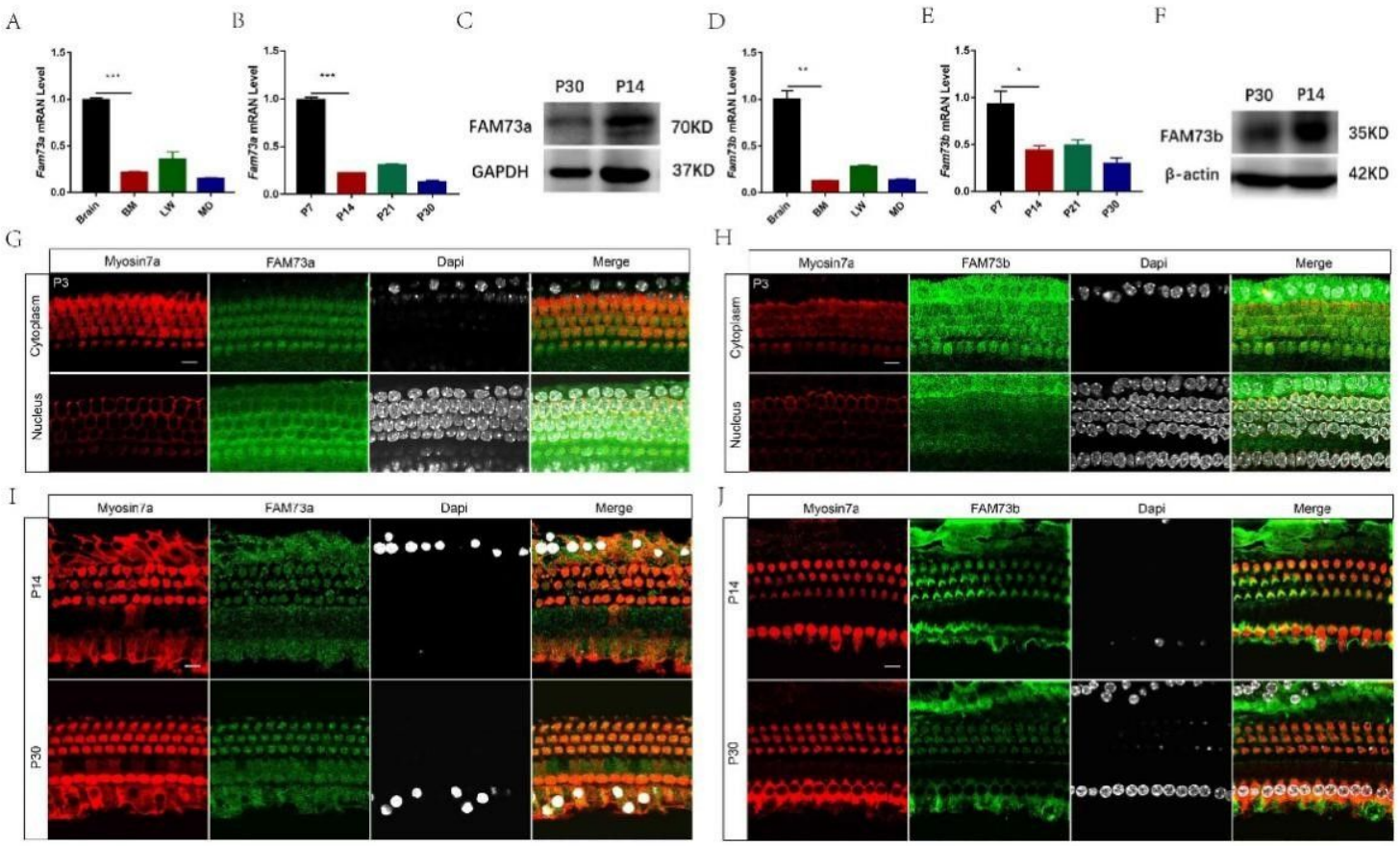

Figure 1

Expression of FAM73a and FAM73b in the cochlea of WT mice. (A,D) qRT-PCR showed that Fam73a and Fam73b were expressed in the brain tissue, basilar membrane (BM), lateral wall (LW), and modiolus (MD). (B,E) qRT-PCR analysis showed the changes in expression of Fam73a and Fam73b in the cochlea during postnatal development. (C,F) Western blots analysis showed the expression of FAM73a and FAM73b in the cochlea. (G-J) Immunofluorescence staining showed that FAM73a and FAM73b were located on the cytoplasm of HCs. Myosin7a was used as a marker for HCs. Scale bar: 10 μm.

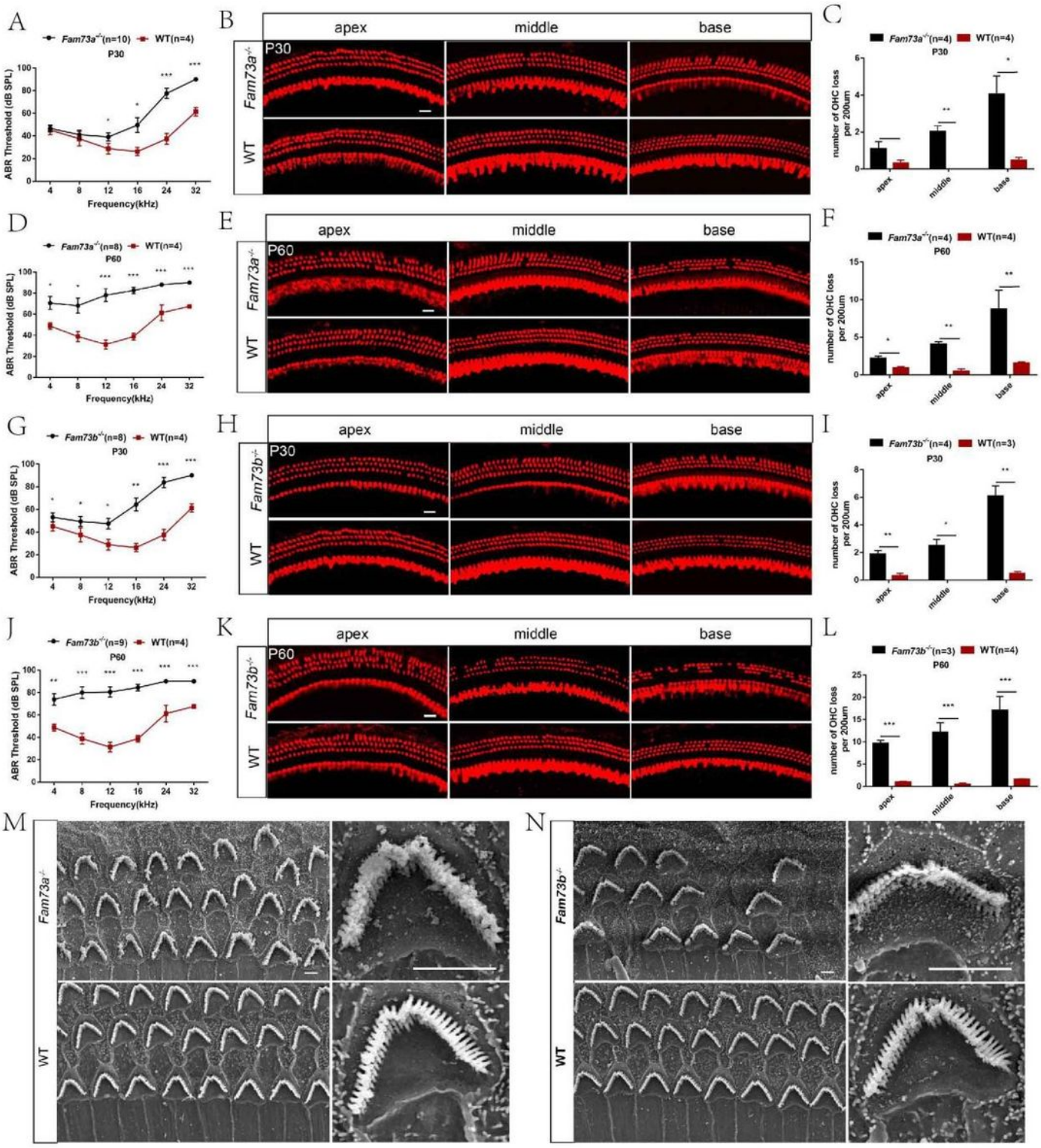

Figure 2

Loss of HCs and destruction of stereocilia structures leads to hearing loss in Fam73a and Fam73b KO mice. (A,D,G,J) Pure-tone ABR thresholds of Fam73a/Fam73b KO mice from P30 to P60 showed progressive hearing loss at 4–32 kHz. (B,E,H,K) Confocal images showed aggravated OHCs loss after staining for Myosin7a in the apical, middle, and basal turns of the cochlea in Fam73a/ Fam73b KO mice from P30 to P60. Scale bars: 20 mm. (C,F,I,L) Comparison of the number of OHCs lost per 200 μm in the

apical, middle, and basal turn of the cochlea in WT and Fam73a/ Fam73b KO mice from P30 to P60 have statistically significant differences. (M,N) The scanning electron microscope images showed the degeneration of cochlear stereociliary bundles from the middle turn of the cochlea in Fam73a/ Fam73b KO mice at P30. Scale bars: 2 mm.

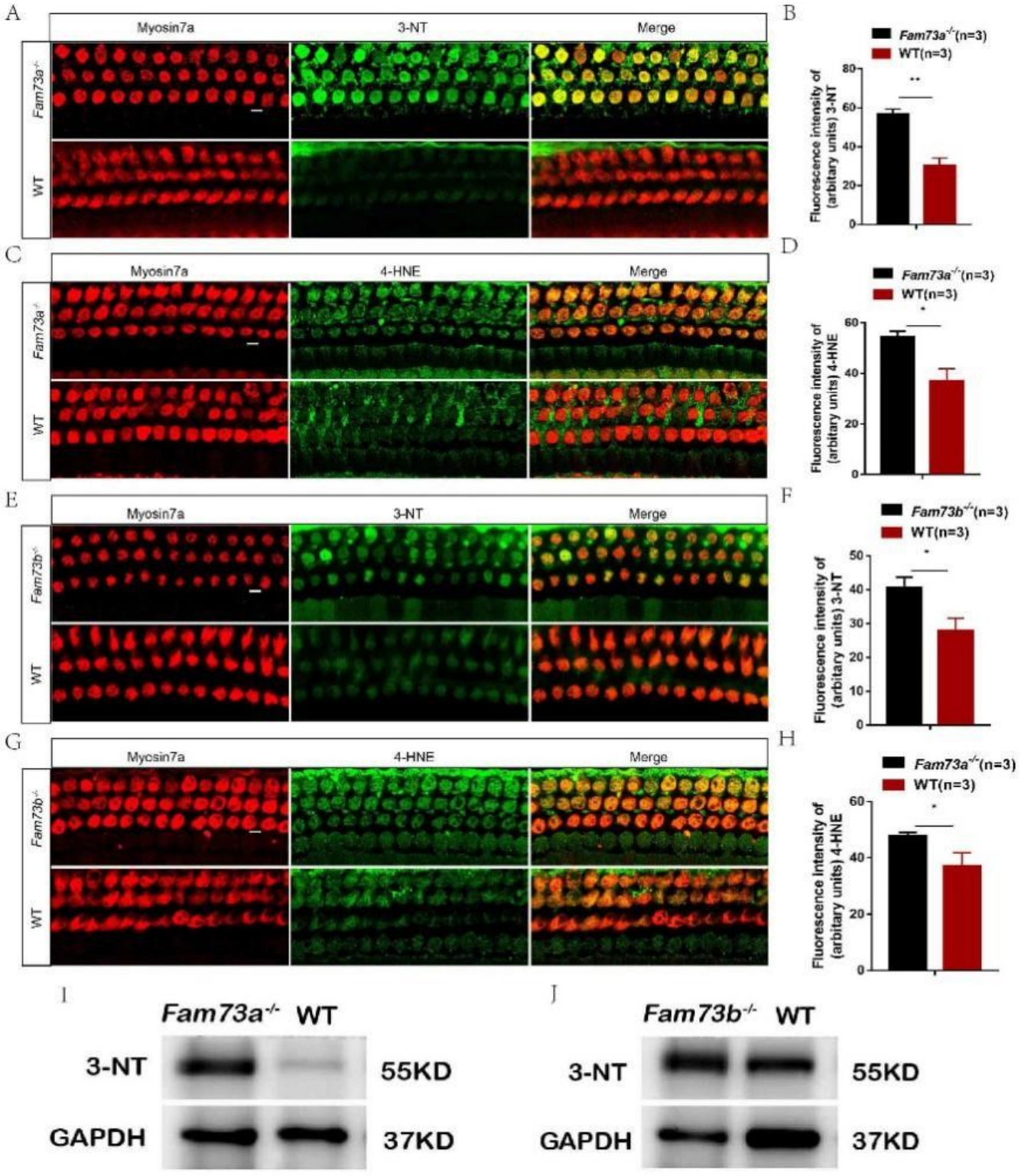

Figure 3

Lack of FAM73a and FAM73b increases oxidative stress in HCs. (A,E) Representative images stained with 3-NT (green) and Myosin7a (red) in OHCs from the basal turn of the cochlea in P21 WT and Fam73a/Fam73b KO mice. (B,F) Quantification of 3-NT immunolabeling in OHCs confirmed a significant increase in P21 Fam73a and Fam73b KO mice. (C,G) Representative images stained with 4-HNE (green) and Myosin7a (red) in OHCs from the basal turn in P21 WT and Fam73a/Fam73b KO mice. (D,H) Quantification of 4-HNE immunolabeling in OHCs confirmed a significant increase in P21 Fam73a and Fam73b KO mice. (I,J) Western blot analysis showed the increased expression of 3-NT in the cochlea of P21 Fam73a/Fam73b KO mice. Scale bar: 2.5 μm.

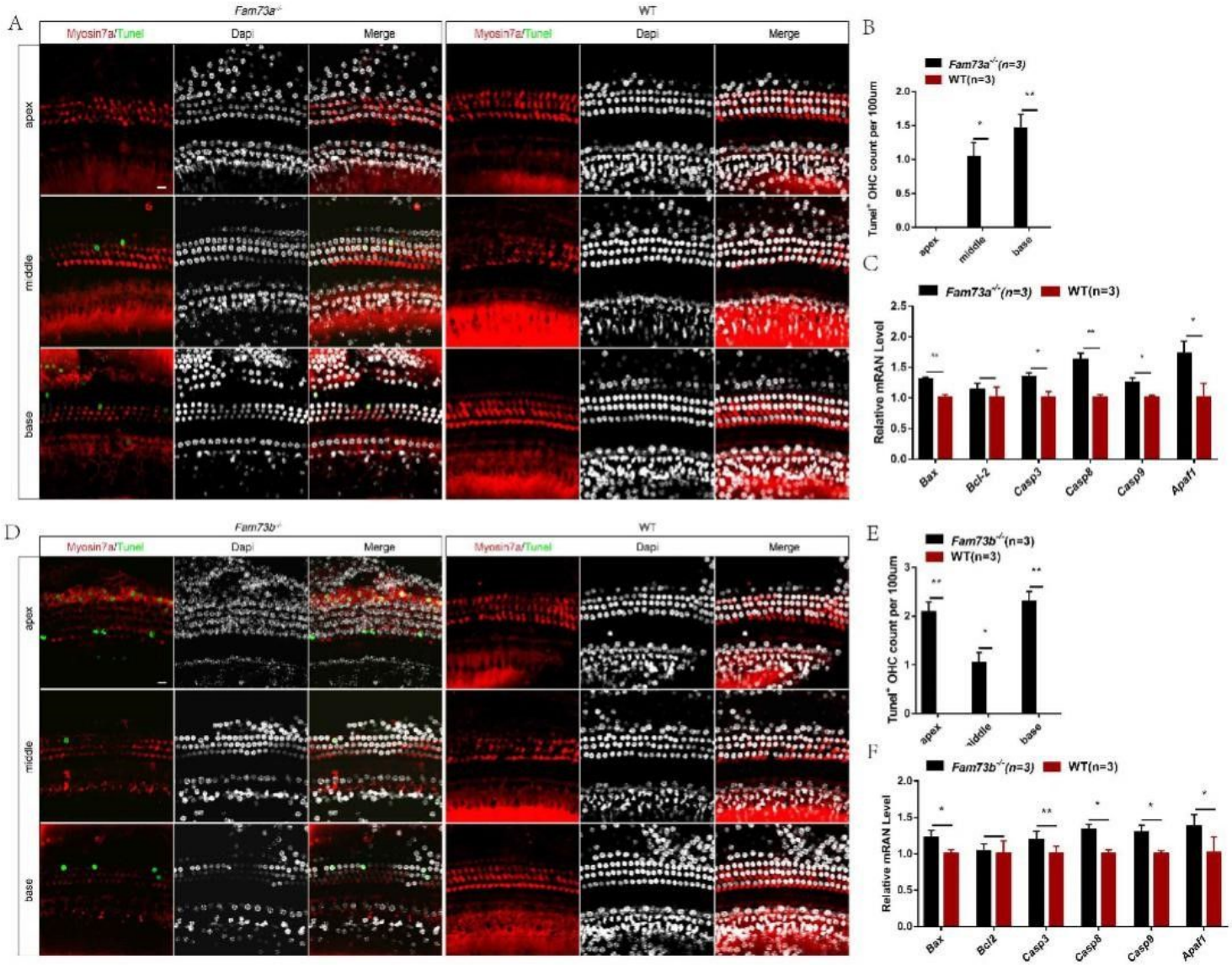

Figure 4

Lack of FAM73a and FAM73b causes apoptosis in HCs. (A,D) Representative images of TUNEL and DAPI double staining showed the apoptotic HCs in the apical, middle, and basal turns of P21 Fam73a/Fam73b KO mice. (B,E) Statistical analysis of the number of TUNEL+ OHCs per 100 μm in the apical, middle, and basal turn showed a significant increase in Fam73a/Fam73b KO mice. (C,F) The mRNA levels of proapoptotic genes and antiapoptotic genes were analyzed by qRT-PCR showed the increased expressin

of proapoptotic marker genes, including Bax, Casp3, Casp8, Casp9, and Apaf1 in the cochlea of P21 Fam73a/Fam73b KO mice. Scale bar: 10 μm.

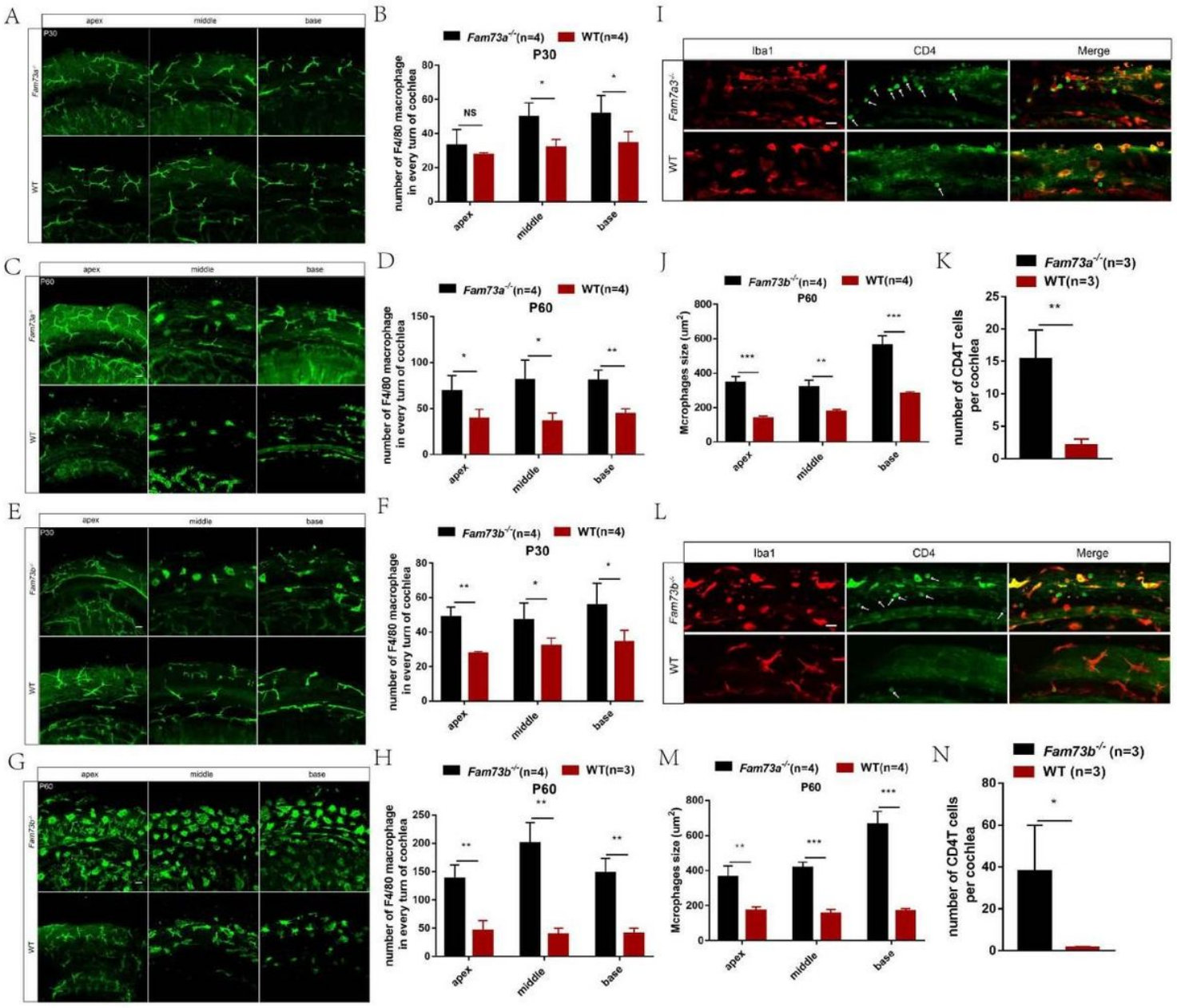

Figure 5

The number of macrophages and CD4+ T cells increase along with changes in macrophage morphology in KO mice. (A,E) Representative images of macrophages in the apical, middle, and basal turns in the basilar membrane showed a increased number in both P30 KO mice except the apical turn of cochlea in Fam73a KO mice. The tissues were stained for F4/80 immunoreactivity. (B,F) Statistical analysis of the numbers of macrophages in the whole length of apical, middle, and basal turns between P30 KO and WT mice was significantly different. (C,G) Representative images of macrophages in the apical, middle, and basal turns in the basilar membrane showed a increased number in both P60 KO mice. (D,H) Comparison of the numbers of macrophages in the whole length of apical, middle, and basal turns between the P60

KO and WT mice have statistically significant differences. (J,M) The sizes of macrophages in the apical, middle, and basal turns were significantly increased in P60 KO mice. (I,L) Representative images of CD4+ T cells in the basilar membrane of the basal turn of the cochlea from P45 KO and WT mice. Macrophages and T cells were stained with Iba1 and CD4, respectively. The white arrows point to CD4+ T cells. (K,N) The numbers of CD4+ T cells in the whole length of the basilar membrane were significantly increased in P45 KO mice. Scale bar: 20 μm.

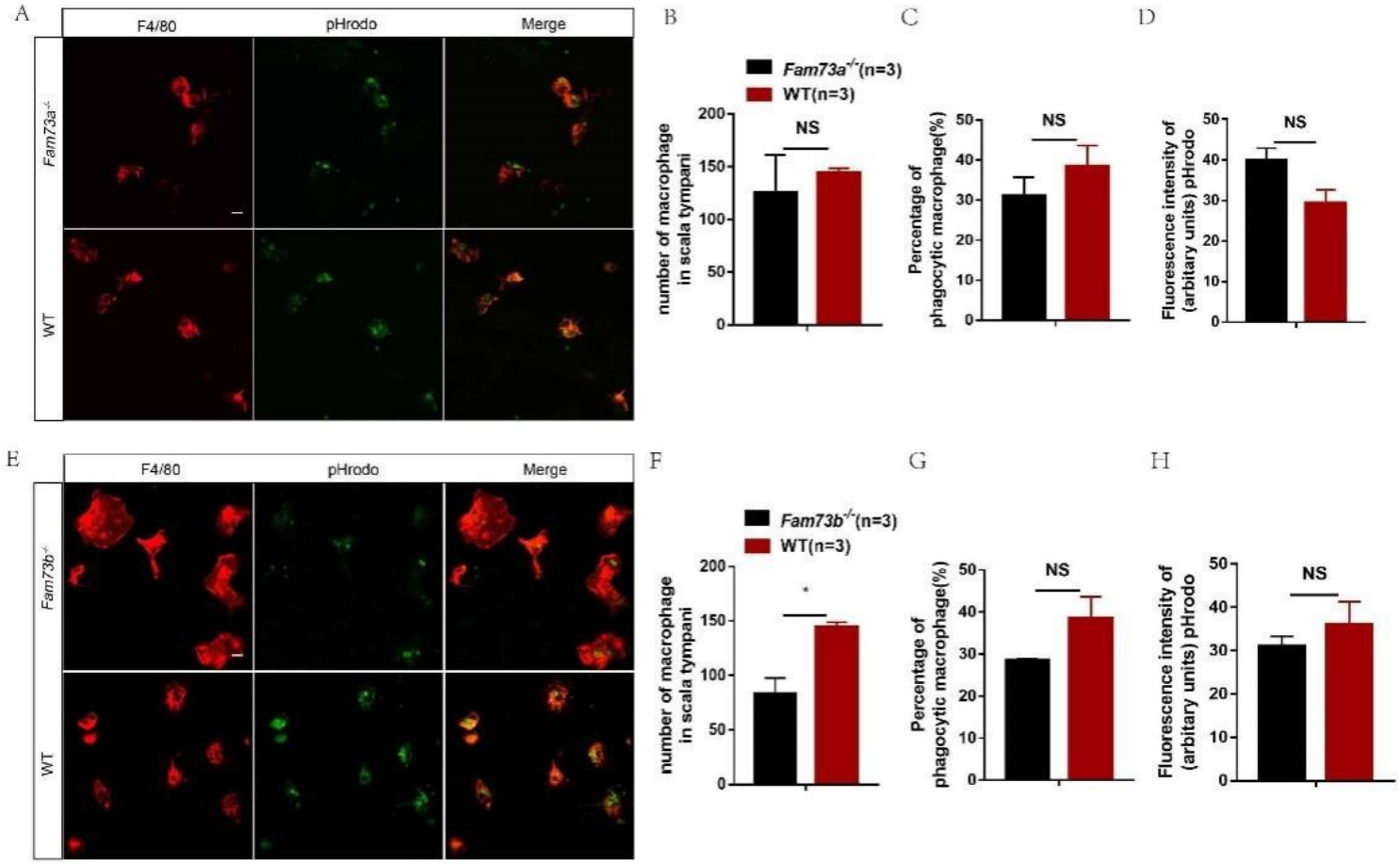

Figure 6

Macrophage phagocytic ability is not significantly changed in Fam73a and Fam73b KO mice. (A,B) Representative images of macrophages phagocytizing pHrodo® bioparticles in P60 WT and Fam73a/Fam73b KO mice. Macrophages stained with F4/80 are red, and pHrodo® bioparticles are green. (B,F) Quantification of the number of macrophages located on the luminal surface of the scala tympani in the basal turn showed no change in Fam73a KO mice and a decreased number in Fam73b KO mice. (C,G) Comparison of the percentage of macrophages phagocytizing pHrodo® bioparticles accounting for all the macrophages on the luminal surface of the scala tympani in P60 WT and Fam73a/Fam73b KO mice showed no significant difference. (D,H) Comparison of fluorescence intensity of pHrodo® bioparticles engulfed by macrophages in P60 WT and Fam73a/Fam73b KO mice showed no significant difference. Scale bar: 10 μm.

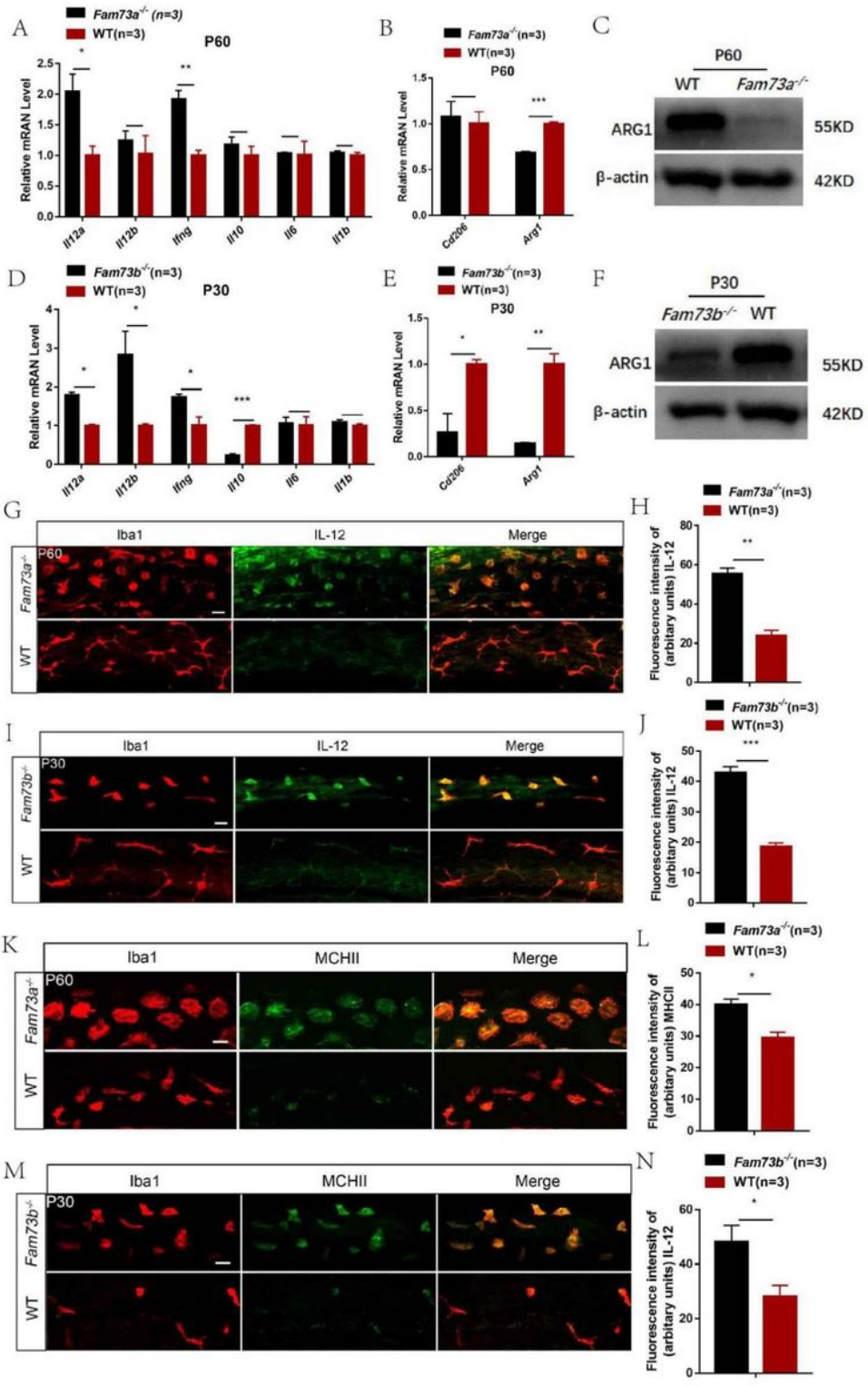

Figure 7

The expression of IL-12, IFN-γ, and MHCII are elevated in Fam73a and Fam73b KO mice. (A,D) The mRNA levels of genes related to proinflammatory cytokines (Il12a, Il12b, Ifng, Il6, Il1b) and anti-inflammatory cytokines (Il10) analyzed by qRT-PCR showed a increased expression of proinflammatory cytokines in Fam73a/Fam73b KO mice. (B,E) qRT-PCR analysis of the M2-type macrophage marker gene (Cd206 and Arg1) confirmed a reduced expression in Fam73a/Fam73b KO mice. (B,E) The reduced protein expression

level of ARG1 was detected by western blot in Fam73a/Fam73b KO mice. (G,I) Immunofluorescence staining with IL-12 and Iba1 antibodies in macrophages of the basilar membrane in WT and Fam73a/Fam73b KO mice. (H,J) Quantification of the fluorescence intensity of IL-12 in (G,I). Fluorescence intensity of IL-12 in KO mice is significantly greater than in WT mice. (K,M) Immunofluorescence staining with MHCII and Iba1 antibodies in macrophages of the basilar membrane in WT and Fam73a/Fam73b KO mice. (L,N) Quantification of the fluorescence intensity of MHCII in (K,M). The fluorescence intensity of MHCII in KO mice is significantly greater than WT mice. Scale bar: 20 μm.

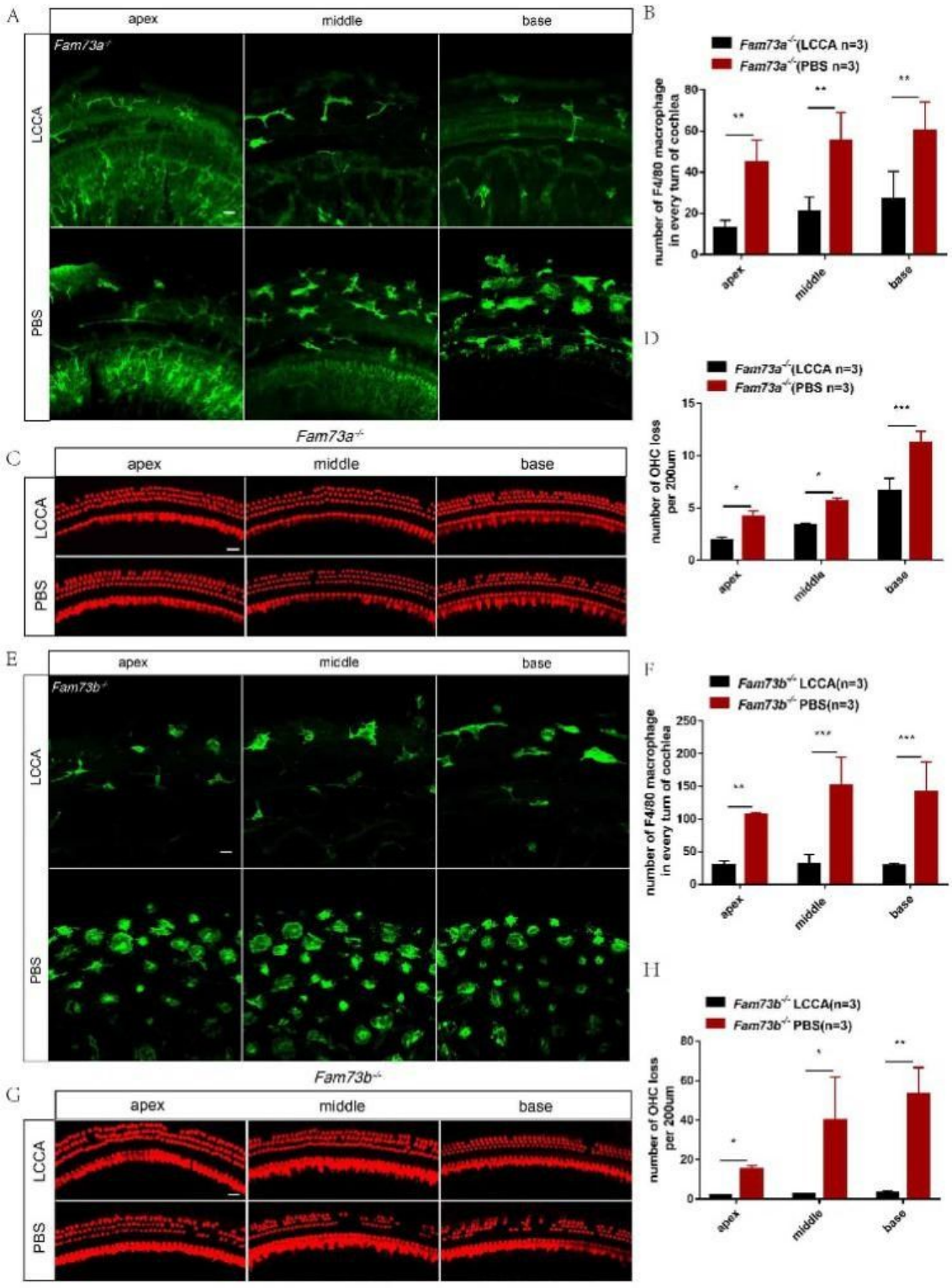

Figure 8

LCCA reduces the number of macrophages and reduces HC loss. (A,E) Representative images of macrophages stained with antibodies against F4/80 in the whole mount basilar membrane of P60 showed a decreased number of macrophages in LCCA-treated KO mice. (B,F) Statistical analysis of the number of macrophages in the apical, middle, and basal turns of LCCA-treated and untreated mice in P60 KO mice show that the differences were statistically significant. (C,G) Representative images of HCs stained with antibodies against Myosin7a in the whole-mount basilar membrane of P60 showed a reduced loss of HCs in LCCA-treated mice KO mice. (D,H) Statistical analysis of the number of OHCs lost per 200 μm in the apical, middle, and basal turns of LCCA-treated and untreated mice in P60 KO mice show that the differences were statistically significant. Scale bar: 20 μm.

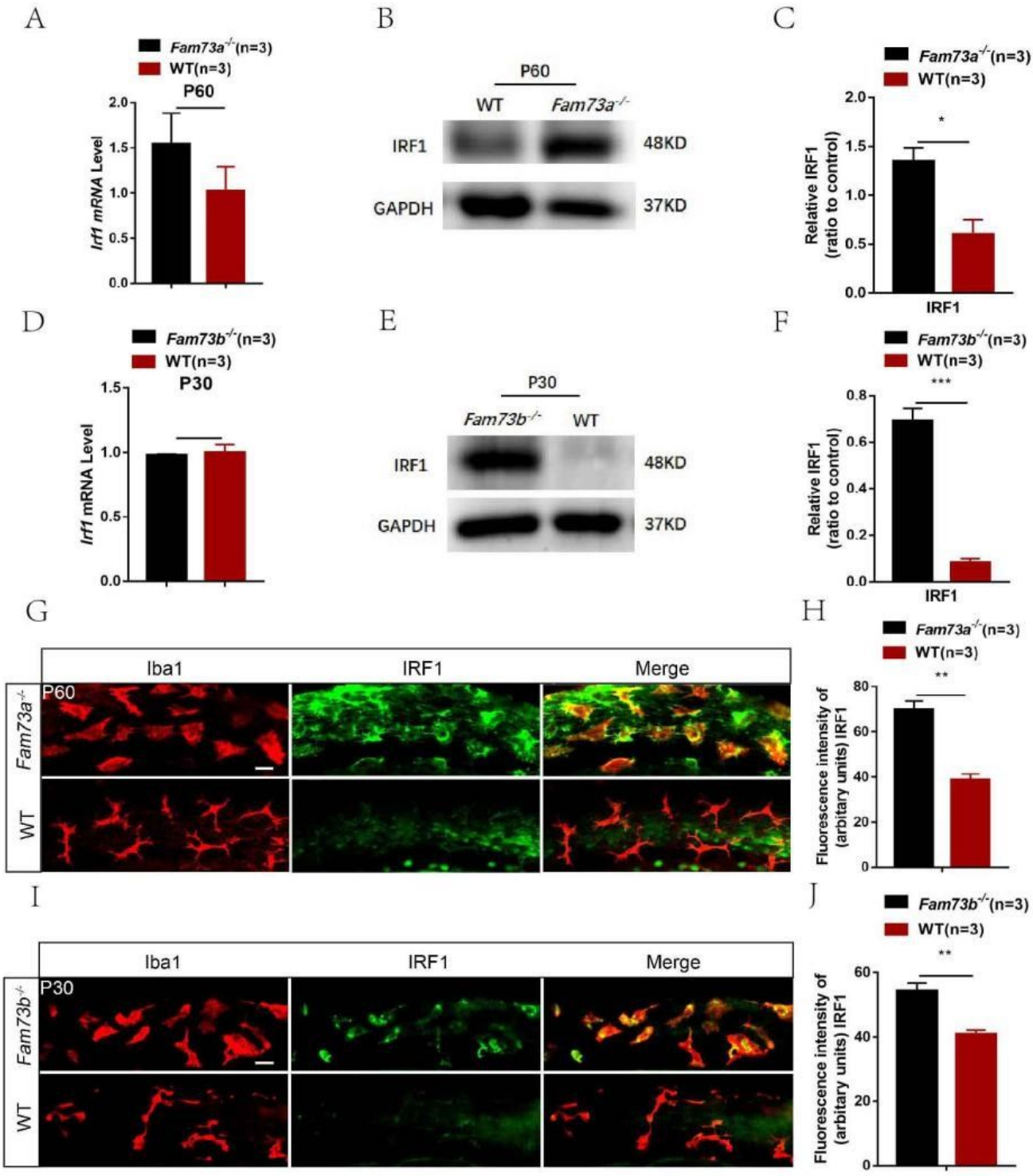

Figure 9

FAM73a and FAM73b deficiency promotes IRF1 accumulation in macrophages. (A,D) The unchanged expression of mRNA level of Irf1 analyzed by qRT-PCR in WT and Fam73a/Fam73b KO mice. (B,E) The increased protein expression of IRF1 analyzed by Western blot in Fam73a/Fam73b KO mice. (C,F) Quantification of the band densities in (B,E) showed that the differences were statistically significant. (G,I) Representative images of macrophages stained with IRF1 (green) and Iba1 (red) in the basilar

membrane of WT and Fam73a/Fam73b KO mice confirmed a increased expression of IRF1. (H,J) Quantification of the fluorescence intensity of IRF1 in (G,I) showed a statistically significant difference between KO and WT mice. Scale bar: 20 μm.

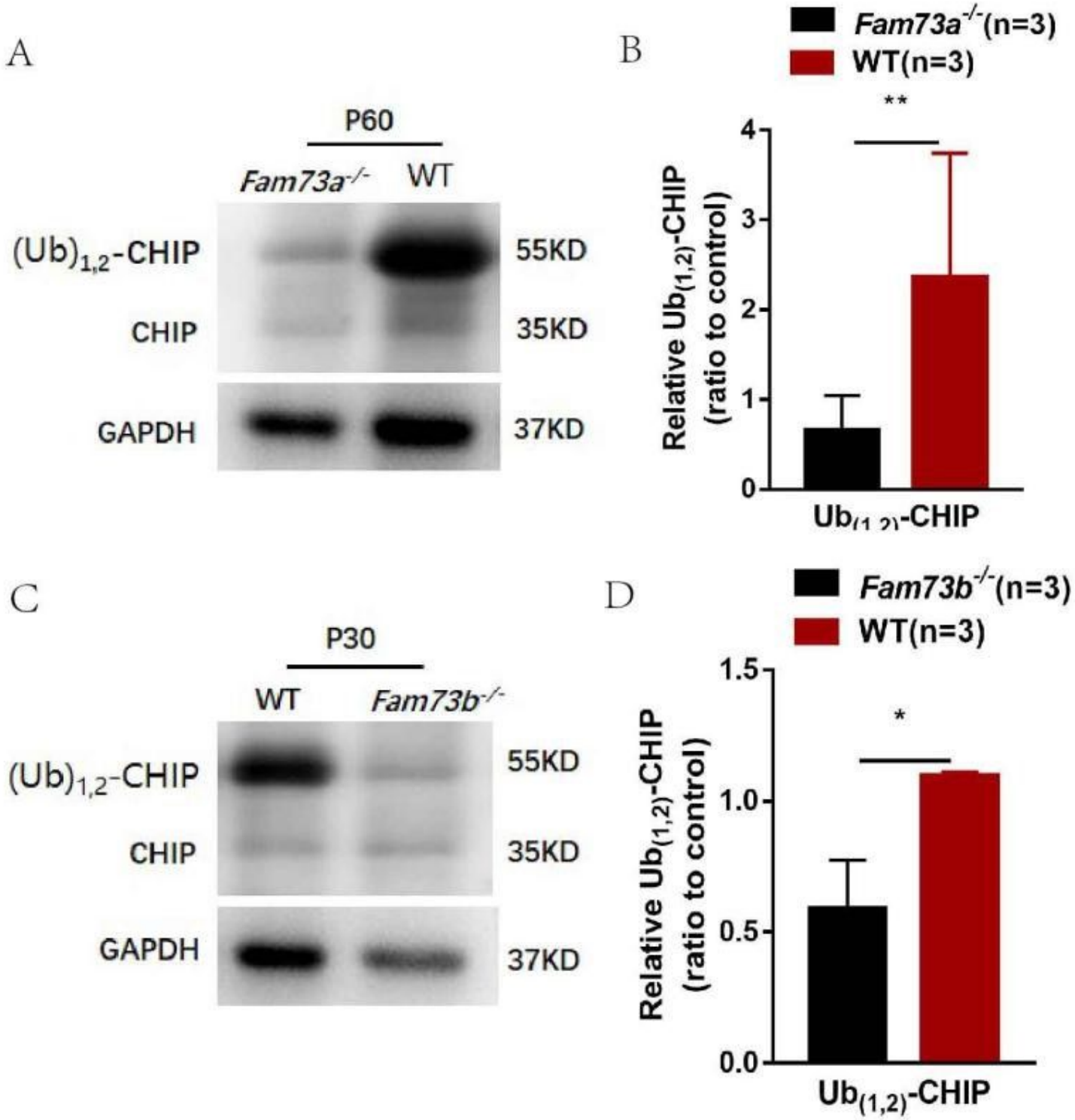

Figure 10

FAM73a and FAM73b deficiency impairs CHIP monoubiquitination in macrophages. (A,C) The increased protein expression of (Ub)1,2-CHIP was detected by IP in Fam73a/Fam73b KO mice. (B,D) Quantification

of band densities in (A,C) showed statistically significant differences between KO and WT mice.

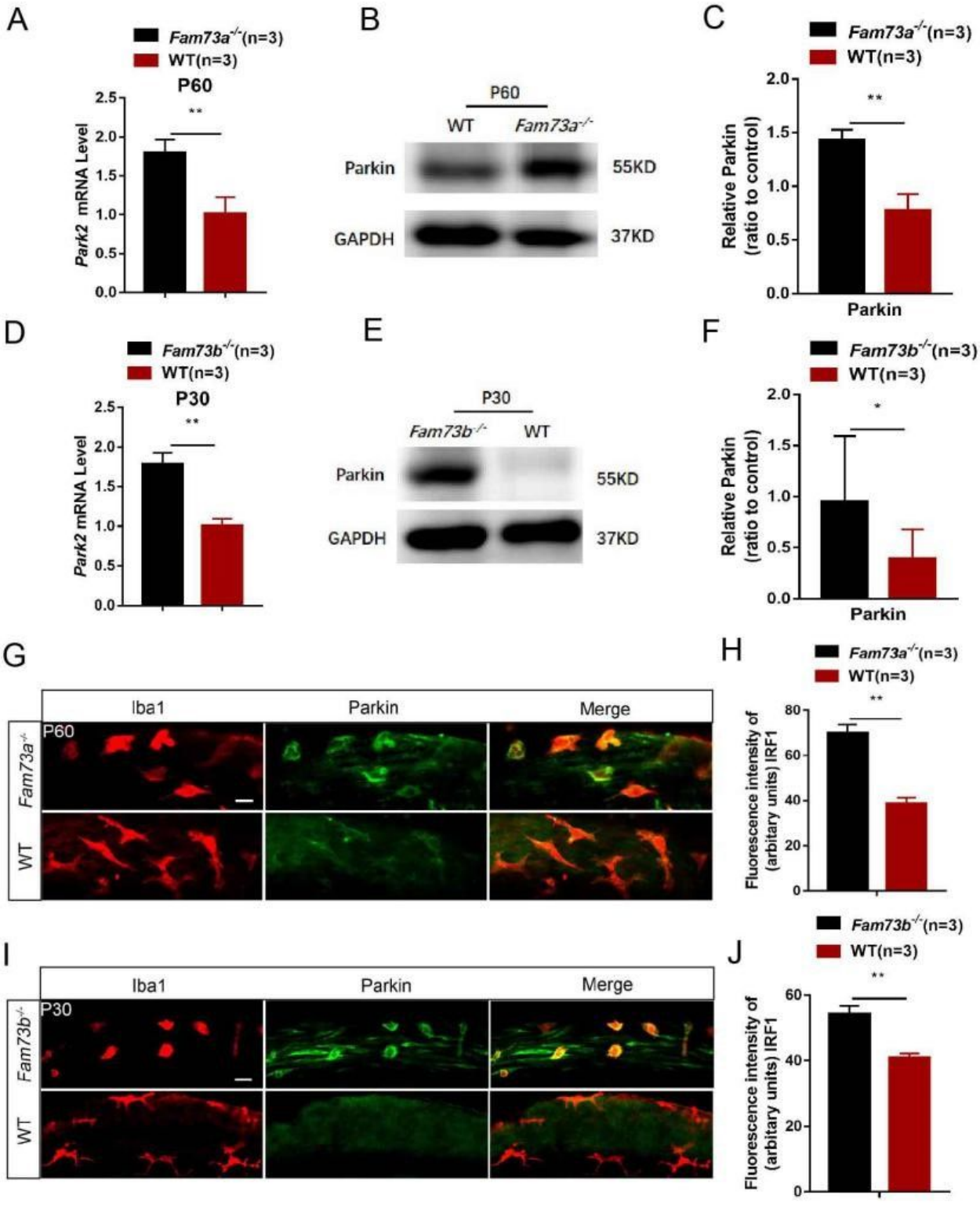

Figure 11

FAM73a and FAM73b deficiency increases Parkin production in macrophages. (A,D) The increased expression of mRNA level of Park2 analyzed by qRT-PCR in Fam73a/Fam73b KO mice. (B,E) Western blot showed the increased protein expression of Parkin in Fam73a/Fam73b KO mice. (C,F) Quantification of band densities in (B,E) showed statistically significant differences between KO and WT mice. (G,I)

Representative images of macrophages stained with antibodies against Parkin (green) and Iba1 (red) in the basilar membrane of WT and Fam73a/Fam73b KO mice confirmed a increased expression of Parkin. (H,J) Quantification of the fluorescence intensity of Parkin in (G,I) showed statistically significant differences between KO and WT mice. Scale bar: 20 μm.

Supplementary Files

This is a list of supplementary files associated with this preprint. Click to download.

- supplement.docx
- GraphicalAbstract.jpeg
- Table.docx